Journal of Pharmacology and Drug Delivery

ScitechJournals

Research Article Open Access

Assessment of Structural and Physicochemical Changes in Thymol and Menthol Induced by Biofield Treatment

Mahendra Kumar Trivedi[1], Shrikant Patil[1], Rakesh K. Mishra[2] and Snehasis Jana[2]*

[1]Trivedi Global Inc., 10624 S EasternAvenue SuiteA-969, Henderson, NV 89052, USA

[2]Trivedi Science Research Laboratory Pvt. Ltd., Hall-A, Chinar Mega Mall, Chinar Fortune City, Hoshangabad Rd., Bhopal-462026, Madhya Pradesh, India

Abstract

Thymol and menthol are naturally occurring plant derived compounds, which have excellent pharmaceutical and antimicrobial applications. The aim of this work was to evaluate the impact of biofield energy on physical and structural characteristics of thymol and menthol. The control and biofield treated compounds (thymol and menthol) were characterized by X-ray diffraction (XRD), Differential Scanning Calorimetry (DSC), Thermogravimetric analysis (TGA), and Fourier Transform Infrared Spectroscopy (FT-IR). XRD study revealed increase in intensity of the XRD peaks of treated thymol, which was correlated to high crystallinity of the treated sample. The treated thymol showed significant increase in crystallite size by 50.01% as compared to control. However, the treated menthol did not show any significant change in crystallite size as compared to control. DSC of treated menthol showed minimal increase in melting temperature (45ºC) as compared to control (44ºC). The enthalpy (ΔH) of both the treated compounds (thymol and menthol) was decreased as compared to control samples which could be due the high energy state of the powders. TGA analysis showed that thermal stability of treated thymol was increased as compared to control; though no change in thermal stability was noticed in treated menthol. FT-IR spectrum of treated thymol showed increase in wave number of –OH stretching vibration peak (14 cm-1) as compared to control. Whereas, the FT-IR spectrum of treated menthol showed appearance of new stretching vibration peaks in the region of 3200-3600 cm^{-1} which may be attributed to the presence of hydrogen bonding in the sample as compared to control. Overall, the result showed that biofield treatment has substantially changed the structural and physical properties of thymol and menthol.

Keywords: Thymol; Menthol; Biofield treatment; XRD; DSC; TGA; FT-IR

Introduction

Thymol is a volatile organic compound extracted from thyme and it has excellent antibacterial properties. Thymol is able to inhibit growth of gram positive microbes such as Bacillus subtilis, Escherichia coli, Klebsiella pneumonia, and Staphylococcus aureus [1]. From last few decades essential oils obtained from herbal products have attracted significant attention as an alternative strategy to replace antibiotic growth promoters. Additionally, thymol has been used in medical [2], food [3-7], agriculture [8] ,veterinarian and pest control applications [9]. Based on recent report, from Word Health Organization, thymol residues can be used in food without danger to the consumer as long as they do not exceed 50 mg/kg and thymol is generally recognized as safe by many national authorities [10]. Researchers have shown that thymol like other phenolic compounds is hydrophobic in nature and it is likely to dissolve in hydrophobic layer of cytoplasmic membrane of bacterial cells, between the lipid acyl chains, thus changing the fluidity and permeability of cell membranes [11]. Based on this excellent property, many research studies showed an additively and synergism of essential oils in combination with antibiotics, indicating that they may offer possibilities of reducing the antibiotic use [12, 13]. However, it has certain disadvantages such as low water solubility and low palatability due to its unpleasant taste and smell [14].

Menthol is cyclic monoterpene alcohol, which is found as a main constituent in essential oil of Mentha candadensis L. (corn mint) and Mentha x piperita vulgaris L. (black peppermint) [15]. Menthol along with menthone, isomenthone and other compounds imparts the cooling minty taste and smell to plants, especially to members of the Mentha genus. Menthol has been included as an ingredient in various consumer products such as pharmaceuticals, cosmetic, pesticide, candies, chewing gums, and other applications [16,17]. Additionally, menthol is known to exhibits antimicrobial, anticancer, and anti-inflammatory activities [18].

Bioelectromagnetism is an area which studies the interaction of living biological cells and electromagnetic fields. Researchers have demonstrated that short lived electrical current or action potential exists in several mammalian cells such as neurons, endocrine cells and muscle cells as well as some plant cells [19]. A physicist, William Tiller proposed the existence of a new force related to human body, in addition to four well known fundamental forces of physics: gravitational force, strong force, weak force, and electromagnetic force. After that biophysicist Fritz-Albert Popp et al. proposed that human physiology shows a high degree of order and stability due to their coherent dynamic states [20-22]. This emits the electromagnetic waves in form of bio-photons, which surrounds the human body and known as biofield energy. Therefore, the biofield consisting of electromagnetic field, generated by moving electrically charged particles (ions, cell, molecule etc.) inside the human body. It is the scientifically preferred term for the biologically produced electromagnetic and subtle energy field that provides regulatory and communication functions within the organism. In spite of countless study reports of the effectiveness of biofield therapies [23], there are very few well controlled experimental studies reported in literature [24].

***Corresponding author:** Jana S, Trivedi Science Research Laboratory Pvt. Ltd., Hall-A, Chinar Mega Mall, Chinar Fortune City, Hoshangabad Rd., Bhopal-462026 Madhya Pradesh, India, Tel: +91-755-6660006; E-mail: publication@trivedisrl.com

Received: August 29, 2025; **Accepted:** October 01, 2025; **Published:** October 09, 2025

Citation: Trivedi MK, Patil S, Mishra RK, Jana S. "Assessment of Structural and Physicochemical Changes in Thymol and Menthol Induced by Biofield Treatment" :109. DOI: 10.59462/JPDD.2.1.109

Thus, human has the ability to harness the energy from environment or universe and can transmit into any leaving or nonliving objects around the globe. The objects always receive the energy and responding into useful way that is called biofield energy and the process is known as biofield treatment. Mr. Mahendra Trivedi is known to transform the characteristics of both living and nonliving materials using his biofield energy. The biofield treatment was used to modify the physical, atomic and thermal properties of various ceramic and metals [25-28]. In agriculture, the biofield treated crops have been reported for significant growth, characteristics and yield of plants [29-31]. Moreover, the biofield has resulted into altered antimicrobials susceptibility patterns and the biochemical characteristics of the microbes [32-34]. The growth and anatomical characteristic of some herbs were also changed after biofield treatment [35-36].

By considering the above mentioned facts and literature on biofield treatment, the present work was undertaken to see the influence of biofield energy on physical and structural properties of thymol and menthol.

Experimental

Materials and methods

Thymol and menthol were procured from S D Fine Chemicals Limited, India. The each sample was divided into two parts; one was kept as a control sample, while the other was subjected to Mr. Trivedi's biofield treatment and coded as treated sample. The treatment group (T1) was in sealed pack and handed over to Mr. Trivedi for biofield treatment under laboratory condition. Mr. Trivedi provided the treatment through his energy transmission process to the treated group without touching the sample. After that, all the samples (control and treated) were characterized with respect to XRD, DSC, TGA, and FTIR analysis.

Characterization

X-ray diffraction (XRD) study: XRD of thymol and menthol (control and treated) powders were analyzed using Philips Holland PW 1710 X-ray diffractometer system. The wavelength of the radiation used in XRD was 1.54056 angstrom. The data was obtained in the form of 2θ versus intensity (a.u) chart. The crystallite size was calculated based on the intense crystalline plane obtained from XRD graph. The obtained data was used to calculate the crystallite size using the following formula:

$$\text{Crystallite size} = k\lambda / b \cos\theta \quad (1)$$

Where λ is the wavelength and k is the equipment constant (0.94).

Differential scanning calorimetry (DSC) study: The thymol and menthol (control and treated) powders were analyzed using a Pyris-6 Perkin Elmer DSC on a heating rate of 10°C/min under air atmosphere.

Thermogravimetric analysis (TGA): Thermal stability of thymol and menthol (control and treated) were analyzed using Metller, Toledo simultaneous TGA and differential thermal analyzer (DTA). The samples were heated from room temperature to 400°C with a heating rate of 5°C/min under air atmosphere**.**

Fourier transform infrared (FT-IR) spectroscopy: The infrared spectra of thymol and menthol (control and treated) were recorded on FT-IR spectrometer, (SHIMADZU, Japan). The FT-IR spectrum was recorded in the range of 4000-500 cm^{-1} .

Results and discussion

XRD study

XRD diffractogram of control and treated thymol are presented in (Figure 1), where, a and b represented to control and treated sample, respectively. The XRD diffractogram of control thymol powder exhibited (Figure 1a) intense crystalline peaks at 2θ equals to 11.50°, 11.78°, 11.95°, 15.77°, 16.47°, 16.62°, 16.82°, 18.71º, 20.30º, 20.76º, 24.01º, 25.35º, 34.24º, and 35.16º. All these peaks demonstrated the crystalline nature of the thymol powder. Whereas the treated thymol (Figure 1b) powder showed increase in intensity of the XRD peaks with 2θ equals to 10.27º, 12.01º, 16.31º, 16.53º, 18.59º, 18.78º, 20.60º, 24.05º, 25.21º, 25.44º, 26.22º, 26.77º, 29.48º, 31.99º, 40.21º, and 40.32º. The closer observation of XRD diffractogram of treated thymol showed increase in intensity of 2θ equals to 25.44º-31.99º XRD peaks as compared to control sample where these peaks were present on lower intensity. Moreover, the 2θ

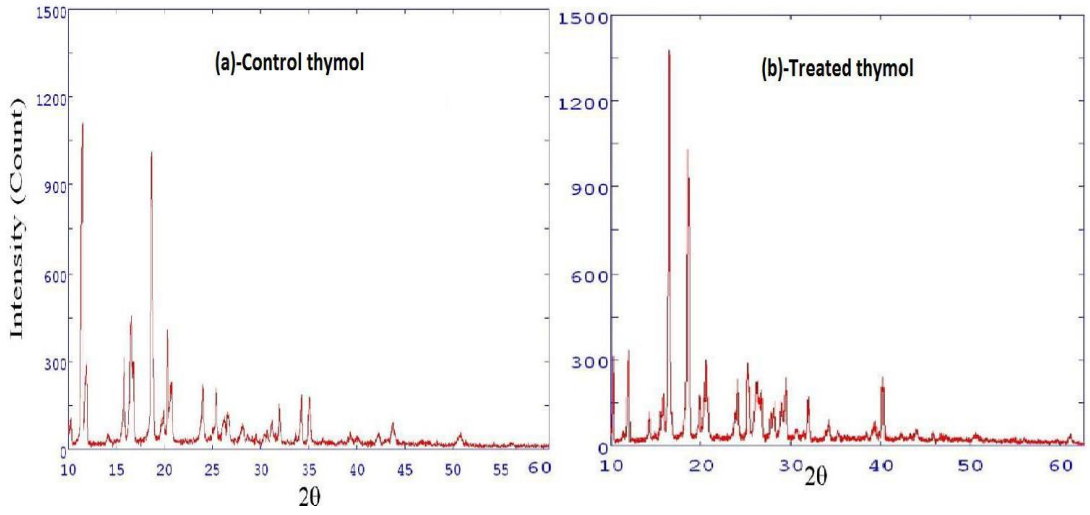

Figure 1: XRD diffractogram of thymol (a) control; (b) treated.

equals to 40.04º XRD peak originally present in control sample with lower intensity, was increased to 2θ equals to 40.21º, 40.32º in treated thymol. This showed the increase in intensity of the XRD peaks which may be correlated to increase crystallinity of the treated sample with respect to control. It is postulated that biofield energy may be acted at atomic level in the treated thymol and induced perfect arrangement in the crystals that caused alteration in crystallinity. It was previously reported that high energy radiation treatment appreciably increases the crystallinity in polyethylene and polytetrafluoroethylene [37-39]. Similarly, in the present work biofield energy might be acted as a cross linker in thymol and led the formation of crystalline entanglements which enhanced the crystallinity.

(Figure 2a and 2b) shows the XRD diffractogram of the control and treated menthol crystals. The control sample showed (Figure 2a) well defined crystalline peaks at 2θ equals to 12.11º, 12.33º, 13.83º, 14.09º, 14.41º, 16.07º, 16.21º, 16.64º, 16.78º, 16.93º, 20.56º, 20.82 º, 24.38º, and 32.74º. Nevertheless, the treated menthol sample showed (Figure 2b) significant change in crystalline peaks at 2θ equals to 12.51º, 14.01º, 14.15º, 16.14º, 16.42º, 17.13º, 21.57º, 21.80º and 28.99º. This showed that biofield has significant effect on changing the crystalline pattern of treated menthol with respect to control.

Crystallite size and percentage change in crystallite size of compounds (thymol and menthol) were calculated from XRD diffractograms using Scherrer formula (crystallite size = kλ /b cos θ) and the results are depicted in (Table 1). The control sample of thymol showed the crystallite size of 46.59 nm however, after biofield treatment the crystallite size was increased up to 69.89 nm. It was observed that treated thymol showed 50.01 % change in crystallite size as compared to control; whereas, the control and treated menthol showed crystallite size 52.23 nm and 52.25 nm, respectively. The treated menthol showed only 0.04 % changes in crystallite size as compared to control sample. It was previously reported that exposure of high temperature and sintering on materials causes impact on corresponding crystallite size. Wijesinghe et al., reported [40] that increase of synthesis temperature has significant impact on crystallite size of hydroxyapatite. Lazic et al., also observed similar results during their studies on hydroxyapatite precipitated from calcium hydroxide and phosphoric acid [41]. Hence in this study, it is assumed that biofield energy may lead to expansion of crystallite size of thymol. Carballo et al., reported that rate of reaction can be significantly improved by increase in crystallite size [42]. Hence, treated thymol due to high crystallite size may improve the reaction rate and percentage yield during synthesis of pharmaceutical compounds.

DSC Study

DSC thermogram of control and treated thymol are presented in Figure 3, where, a and b represented to control and treated sample, respectively. The thermogram of control thymol showed the endothermic peak at 148ºC which could be due to oxidation of the compound (Figure 3a). DSC thermogram showed another endothermic peak at 125ºC that could be due to oxidation of the treated sample (Figure 3b).

(Figure 4a and 4b) shows the DSC thermogram of control and treated menthol crystals, respectively. The typical DSC thermogram of control menthol exhibited a melting endothermic transition temperature at 44ºC which was similar to previously reported melting temperature of menthol [43]. Another endothermic peak was observed in control menthol at 138ºC which was possibly due to thermal oxidation of the sample (Figure 4a). Whereas the biofield treated menthol showed a melting peak at 45ºC which showed increase in melting temperature as compared to control (Figure 4b). It showed that biofield treatment may induced symmetrical or regular arrangement in the menthol crystals. Though the DSC thermogram of treated menthol showed lower thermal oxidation temperature, 107ºC as compared to control sample. The enthalpy (ΔH; J/g) was computed from corresponding DSC thermograms of control and treated organic compounds and depicted in (Table 2) (thymol and menthol). The control thymol showed the ΔH; 183.53 J/g however the treated sample showed decrease in ΔH; 167.49 J/g. However, the control menthol showed the ΔH; 279.84 J/g though decreased ΔH; 145.46 J/g was observed in treated sample. The percentage change in ΔH of treated thymol and menthol was 8.74 % and 48.02 %, respectively. The marked decrease in ΔH of treated thymol and menthol as compared to control might be due to the high energy state of biofield treated samples.

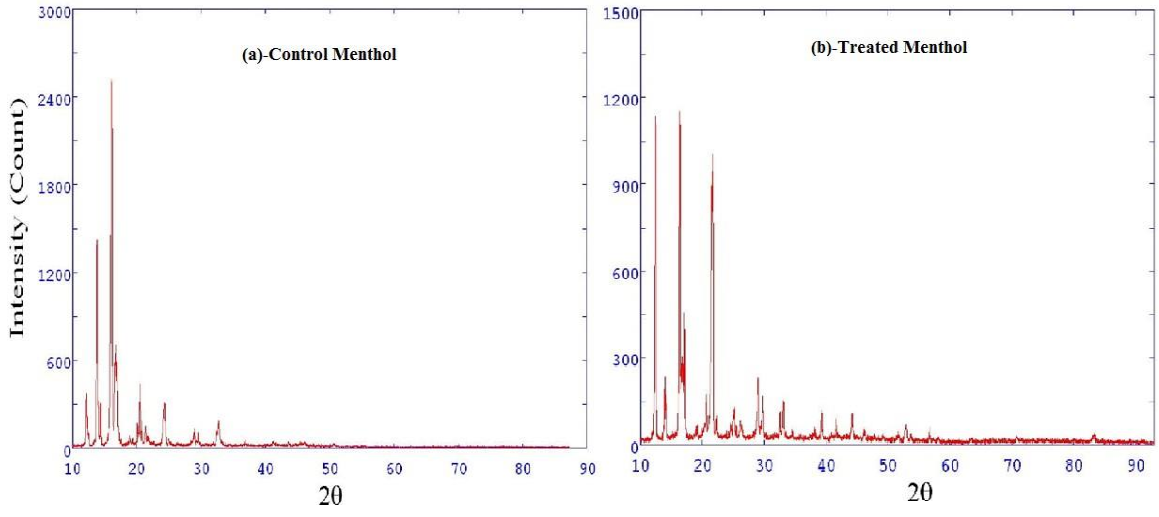

Figure 2: XRD diffractogram of menthol (a) control; (b) treated.

TGA Study

TGA was used to further confirm the thermal stability of control and treated samples of thymol and menthol. The thermogram of control and treated samples are depicted in (Figure 5 and 6), respectively. The TGA thermogram of control thymol showed one step thermal degradation pattern. The control thymol showed (Figure 5) onset temperature at 142ºC and thermal degradation ended at around 186ºC. During this thermal event control thymol showed major weight loss of 52.98%. DTA thermogram of control thymol showed an endothermic peak between 40-60ºC, probably associated with dehydration and melting of the sample. DTA curve showed another endothermic peak at 170ºC, which was associated with thermal degradation of the control. Based on derivative thermogravimetry (DTG) the maximum thermal decomposition was noticed at 160ºC. The TGA thermogram of treated thymol showed identical thermal degradation pattern as showed by the control sample (Figure 6). Treated thymol showed late onset at 152ºC as compared to control and the degradation stopped at 192ºC. During this process the treated thymol lost 43.82% of its weight. The DTA thermogram of treated thymol showed thermal changes or melting as displayed by its endothermic peak at 54ºC. Another endothermic peak was observed at 175ºC which was possibly due to thermal degradation or oxidation of the sample and this peak was found to be 5ºC higher as compared to control. Additionally, the DTG curve showed significant increase in maximum thermal decomposition temperature, 166ºC of the treated thymol. Altogether, TGA, DTA and DTG data provided sufficient evidence that thermal stability of thymol was increased after biofield treatment as compared to control. The increase in thermal

Sample	Crystallite size (nm)		% Change in crystallite size
	Control	Treated	
Thymol	46.59	69.89	50.01
Menthol	52.23	52.25	0.04

Table 1: Crystallite size and percentage change in crystallite size of thymol and menthol.

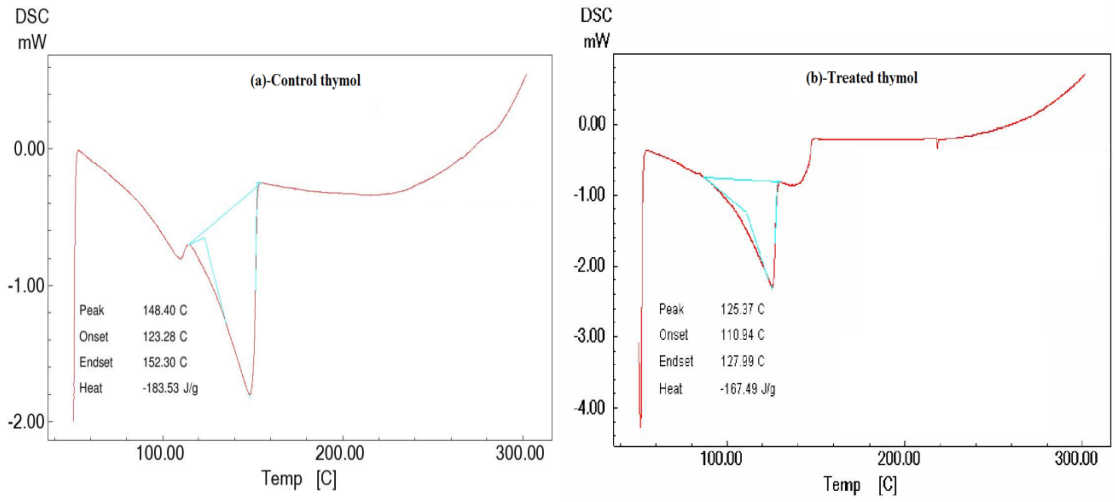

Figure 3: DSC thermogram of thymol (a) control; (b) treated.

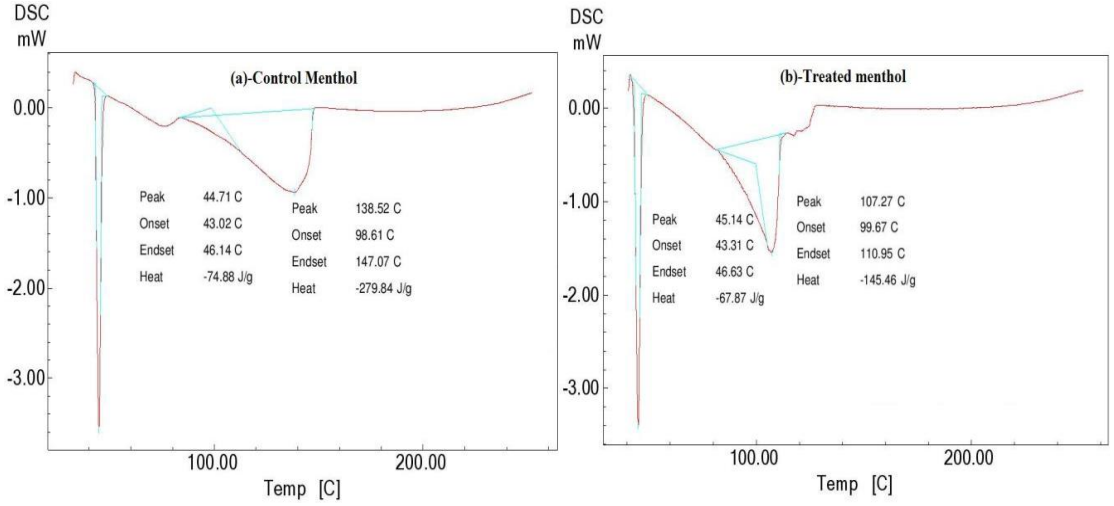

Figure 4: DSC thermogram of menthol (a) control; (b) treated.

stability of treated thymol was may be due to conformational changes and crosslinking caused by biofield treatment [44].

(Figure 7 and 8) shows the TGA thermogram of control and treated menthol. The control menthol thermogram showed one step thermal degradation pattern. It showed an onset temperature at 120ºC and thermal degradation eventually ended at 165ºC. The control menthol showed rapid weight loss during this process (48.46%) and this probably occurred due to oxidation of the sample (Figure 7). DTA thermogram of control showed a small endothermic peak between 45-50ºC which was due to melting of the sample. The second endothermic peak in DTA at 148ºC was may due to thermal oxidation or degradation of the compound. Based on DTG curve the maximum thermal decomposition temperature of control menthol was at 138ºC. Whereas, the TGA thermogram of treated menthol showed (Figure 8) an onset temperature at 120ºC and thermal degradation was terminated at 160ºC. The DTA curve of treated menthol showed no melting peak and second endothermic peak was observed at 148ºC. DTG curve of treated menthol showed similar maximum thermal decomposition temperature at 138ºC as showed by the control. Hence, the TGA, DTA and DTG thermogram showed that thermal stability of treated menthol did not alter after biofield treatment.

Table 2: Enthalpy (ΔH) change in control and treated compounds (thymol and menthol).

Sample	Control (ΔH J/g)	Treated (ΔH J/g)	% Change in ΔH
Thymol	-183.53	-167.49	-8.74
Menthol	-279.84	-145.46	-48.02

FT-IR Spectroscopy

(Figure 9 and Figure 10) shows the FT-IR spectrum of control and treated thymol. The FT-IR spectrum of control thymol showed the vibration peak at 3036 cm^{-1}, 3066 cm^{-1}, 3103 and 3169 cm^{-1} which were attributed due to =C⊠H stretches of armomatics. The spectrum showed (Figure 9) a methyl group streatching peak at 2929 cm^{-1} and stretching peak at 3201 cm^{-1} was due to –OH group. The characteristic C=C stretches in aromatics was observed at 1622 cm^{-1}, 1585 cm^{-1}, and 1458 cm^{-1}. The in plane C⊠H bending was observed at 1091 cm^{-1} and 1058 cm^{-1}. The FT-IR spectrum of treated thymol showed stretching peak for the typical =C⊠H group at 3034 and 3101 cm^{-1}. The treated thymol showed (3215 cm^{-1}) increase in –OH group stretching wavenumber by 14 cm^{-1} as compared to control (3201 cm^{-1}). The increase in –OH stretching wavenumber may due to biofield treatment which could induce structural changes in the treated thymol (Figure 10).

(Figure 11 and 12) shows the FT-IR spectrum of the control and treated menthol, repectively. The FT-IR of control menthol an cyclic monoterpene showed streatching vibration peaks at 3201-3281 cm^{-1} which was due to –OH/phenolic group. The stretching vibration peaks of methyl groups was evident (Figure 11) at 2908, 2953 cm^{-1} and the isopropyl group stretching vibration was observed at 1367 cm^{-1}. All these peaks confirmed the structure of the control menthol [45]. The FT-IR spectrum of treated menthol showed (Figure 12) occurance of these above mentioned IR stretching vibration peaks however, it also showed an increase in intensity of the methyl (⊠CH_3) group stretching and the peaks were obsorved at 2870, 2910, 2933 and 2953 cm^{-1}. The FTIR spectrum also showed emergence of new peaks between 3200-3600 cm^{-1} which was possibly due to hydrogen bonded –OH group stretching

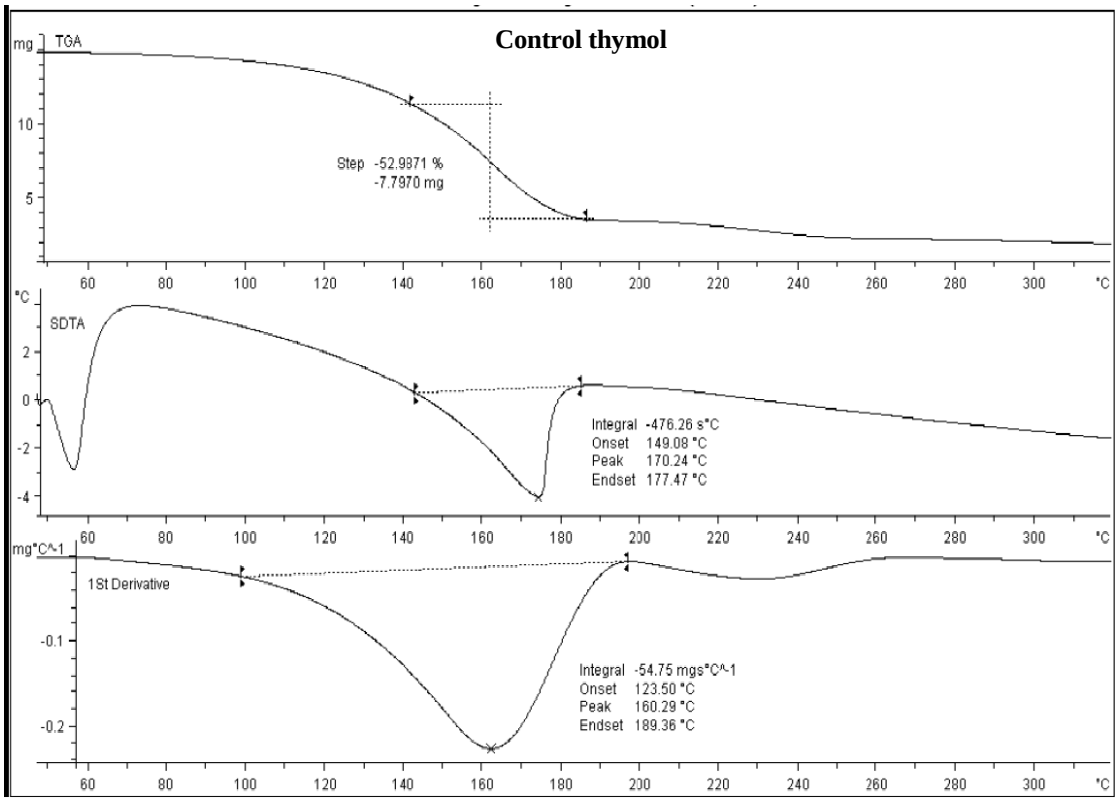

Figure 5: TGA thermogram of control thymol.

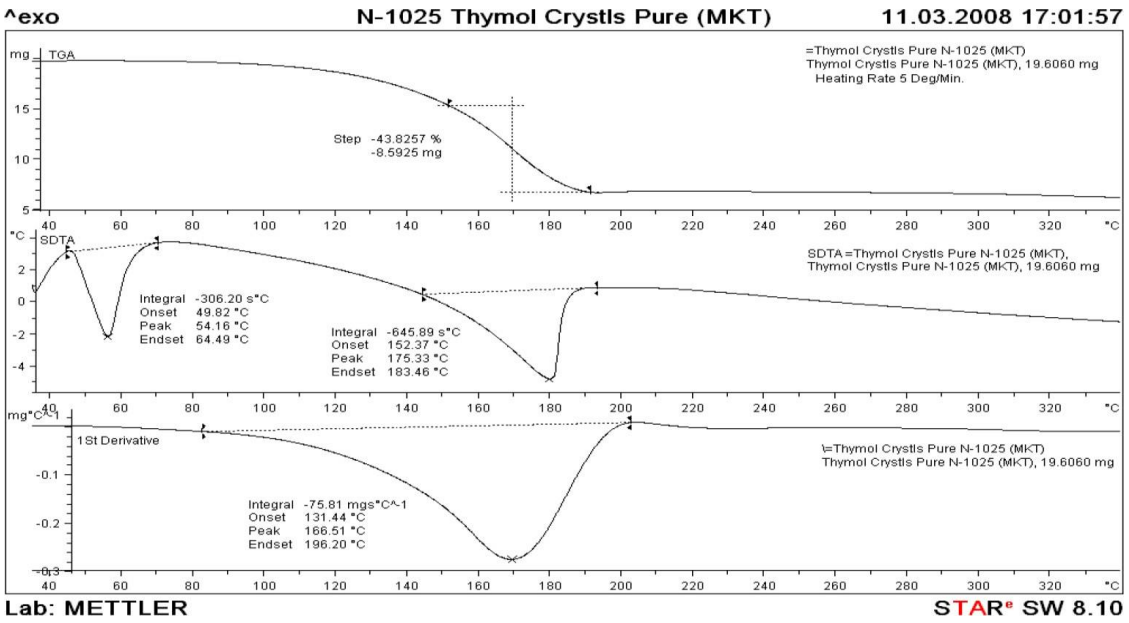

Figure 6: TGA thermogram of treated thymol.

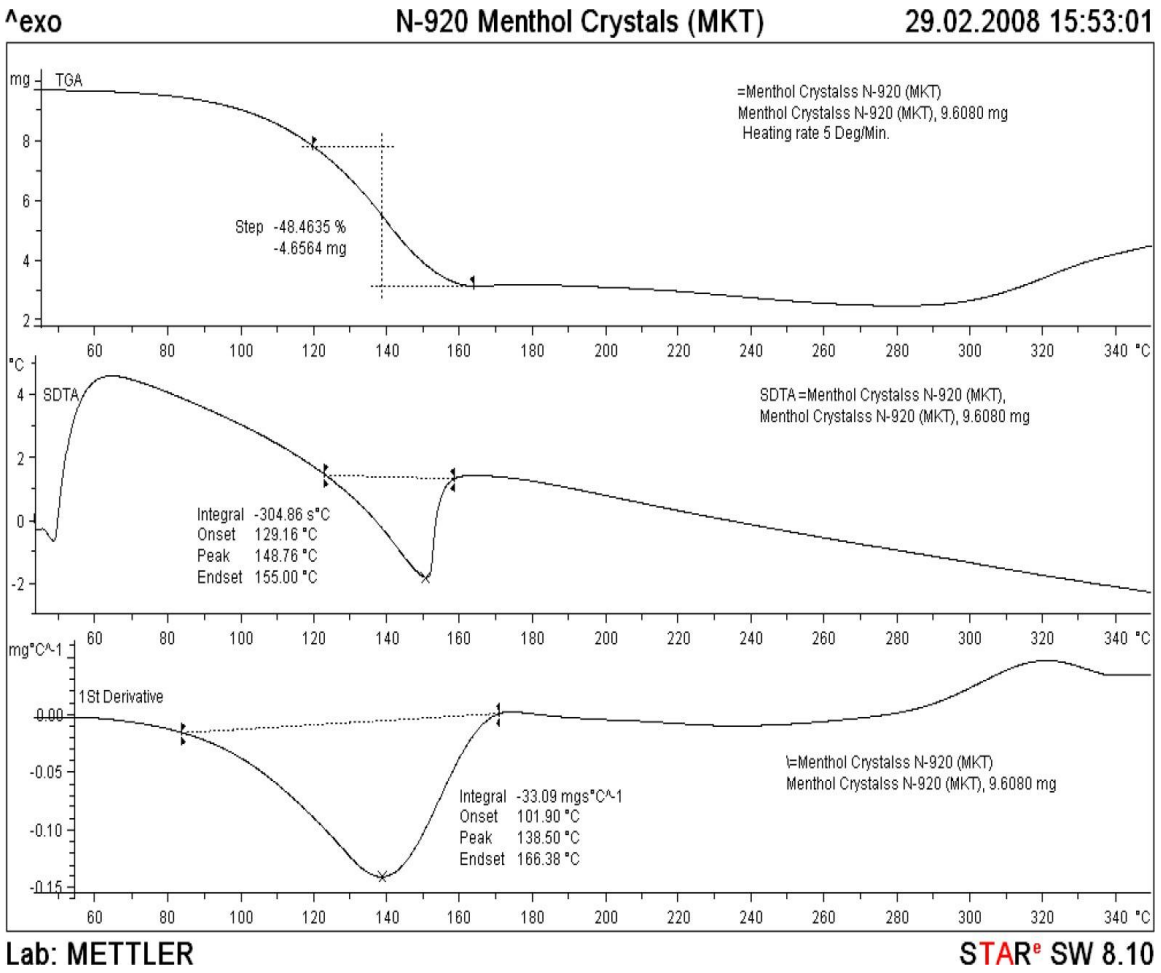

Figure 7: TGA thermogram of control menthol.

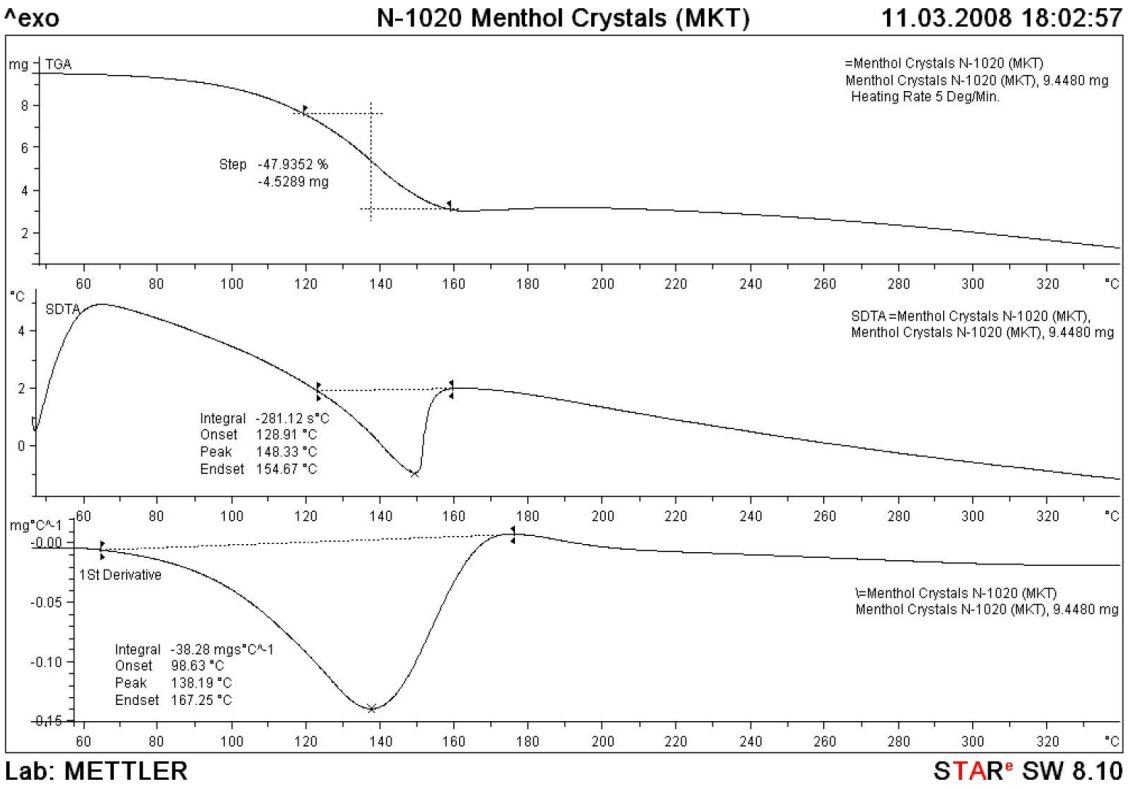

Figure 8: TGA thermogram of treated menthol.

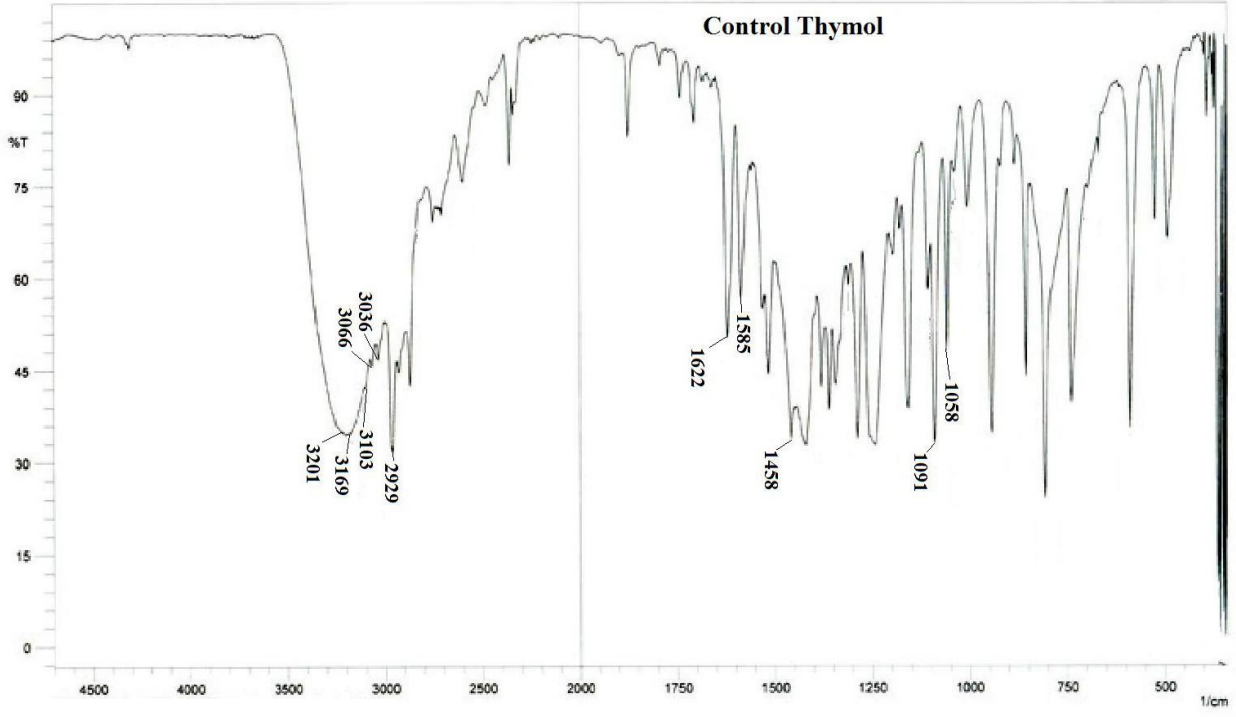

Figure 9: FT-IR spectrum of control thymol.

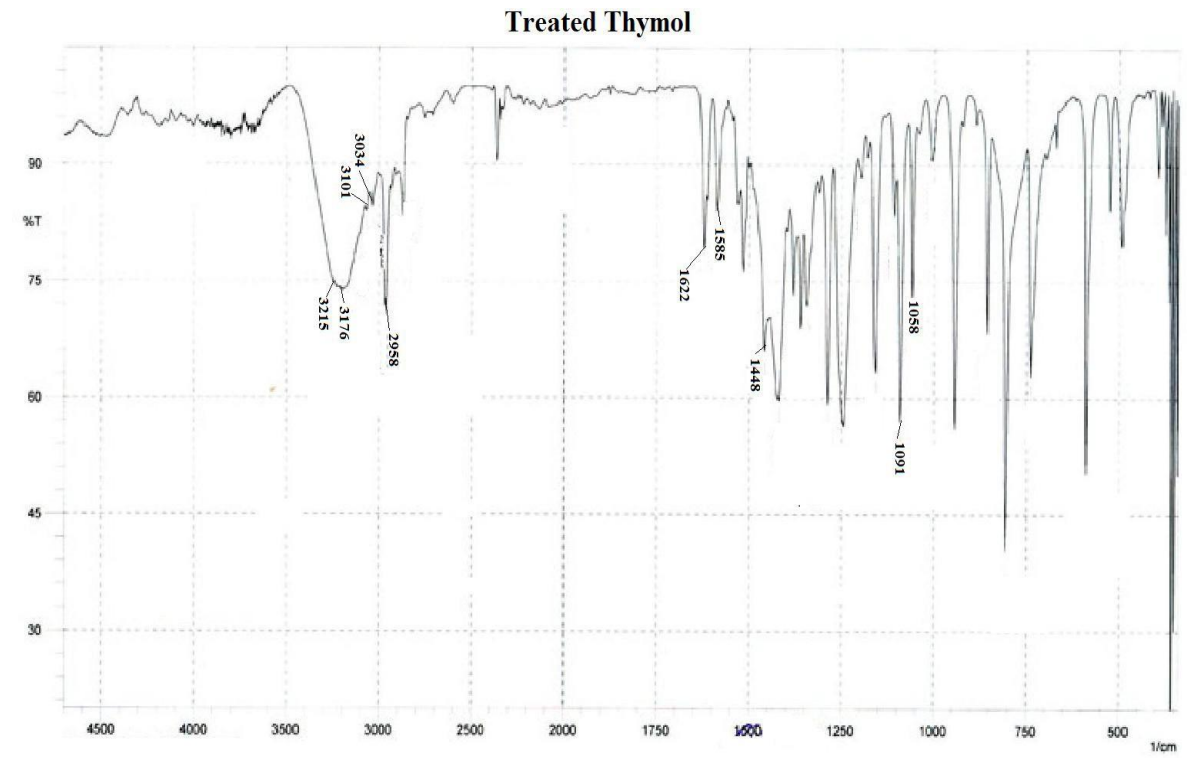

Figure 10: FT-IR spectrum of treated thymol.

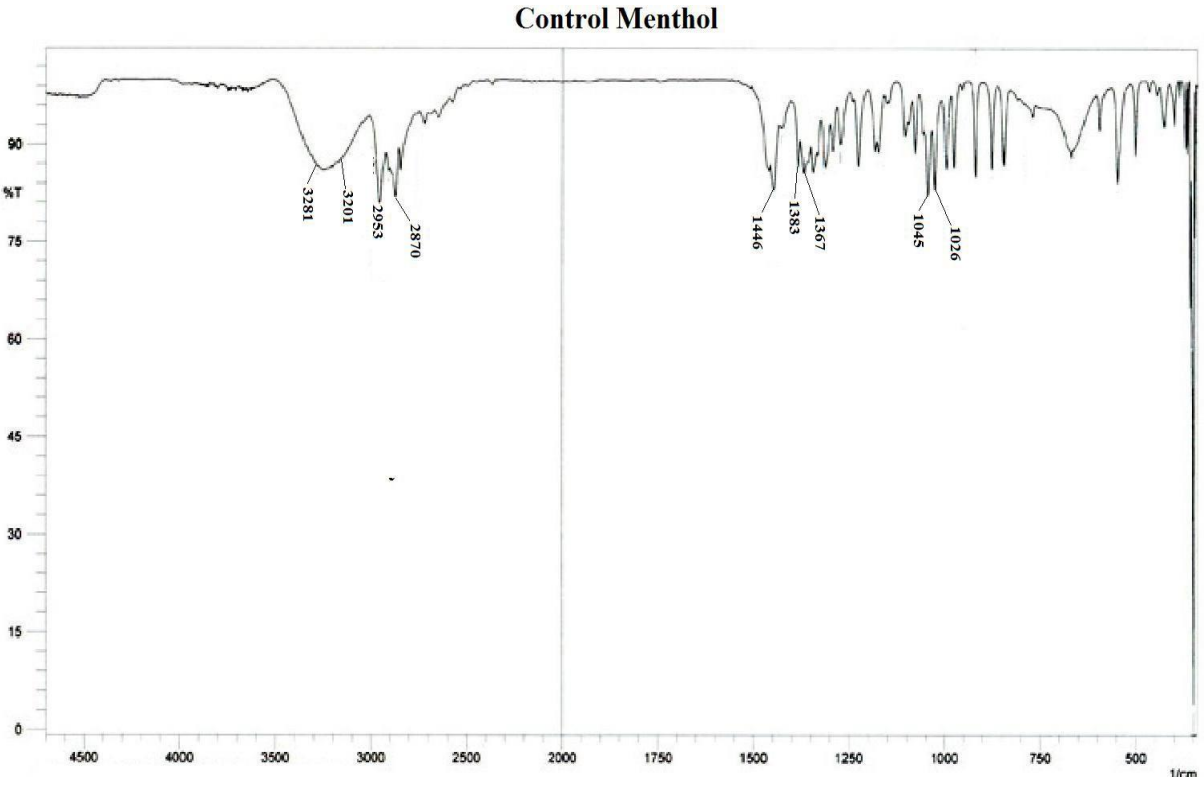

Figure 11: FT-IR spectrum of control menthol.

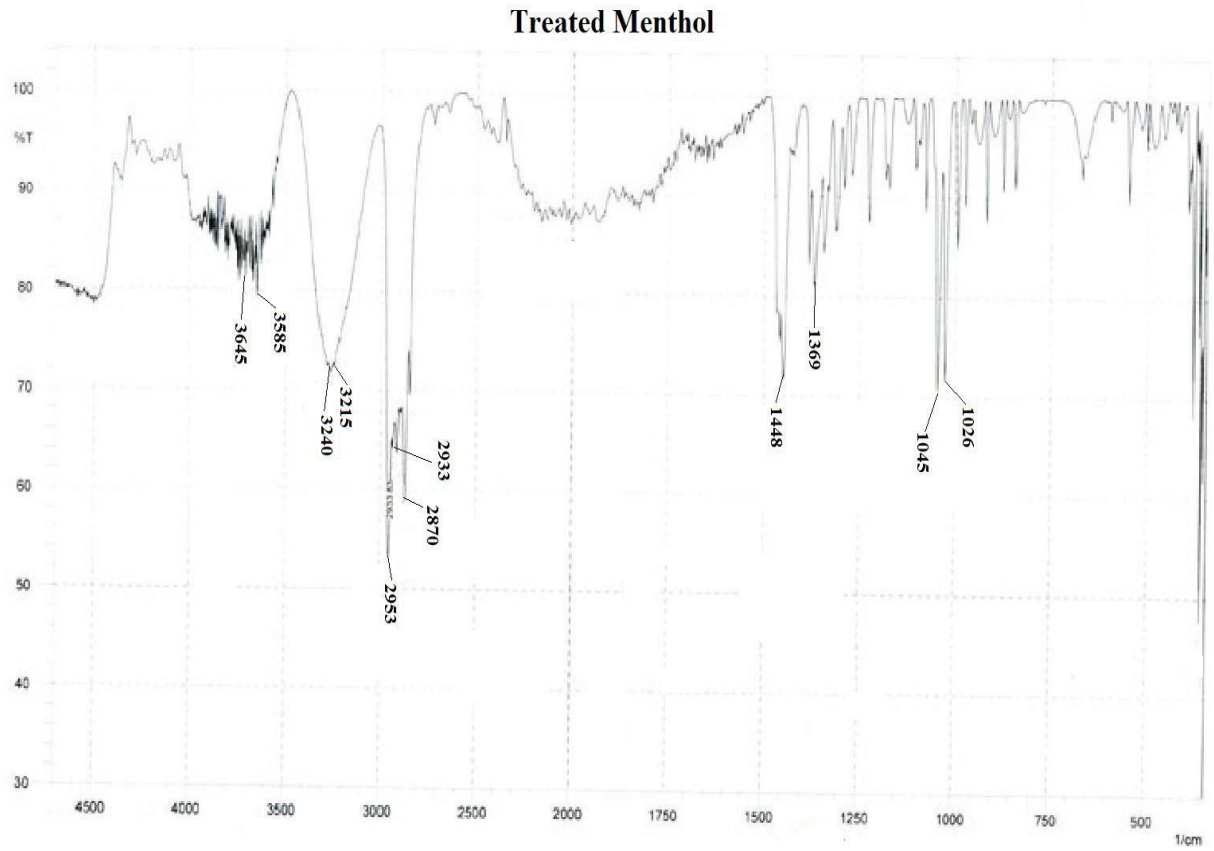

Figure 12: FT-IR spectrum of treated menthol.

in the treated menthol. Hence, it is postulated that emergence of these new peaks might be due to biofield treatment which induced hydrogen bonding in the treated monoterpene.

Conclusion

This study evaluated the impact of biofield treatment on structural, crystalline and thermal properties of two monoterpenes (thymol and menthol). XRD analysis revealed that biofield treatment has increased in crystallite size of treated thymol as compared to control. However, treated menthol showed no significant change in crystal size. Moreover, biofield has induced structural and thermal changes in the treated thymol and menthol. The high crystallite size and good thermal stability of thymol may substantially increase the rate of reaction and it could improve the reaction yield during synthesis of pharmaceutical compounds. It could be used as novel, cost effective and efficient approach to modulate the physicochemical properties of these compounds. Based on the obtained results it is presumed that the biofield treated monoterpenes (thymol and menthol) could be used as antimicrobial agents for pharmaceutical applications.

Acknowledgement

The authors would like to thank all the laboratory staff of MGV Pharmacy College, Nashik for their assistance during the various instrument characterizations. We thank Dr. Cheng Dong of NLSC, institute of physics, and Chinese academy of sciences for permitting us to use Powder X software for analyzing XRD results.

References

1. Dorman HJ, Deans SG (2000) Antimicrobial agents from plants: antibacterial activity of plant volatile oils. J Appl Microbiol 88: 308-316.
2. Mendes Ada S, Daemon E, Monteiro CM, Maturano R, Brito FC, et al. (2011) Acaricidal activity of thymol on larvae and nymphs of *Amblyommaca jennense* (Acari: Ixodidae). Vet Parasitol 183: 136-139.
3. Evans JD, Martin SA (2000) Effects of thymol on ruminal microorganisms. Curr Microbiol 41: 336-340.
4. Lambert RJ, Skandamis PN, Coote PJ, Nychas GJ (2001) A study of the minimum inhibitory concentration and mode of action of oregano essential oil, thymol and carvacrol. J Appl Microbiol 91: 453-462.
5. Sacchetti G, Maietti S, Muzzoli M, Scaglianti M, Manfredini S, et al. (2005) Comparative evaluation of 11 essential oils of different origin as functional antioxidants, antiradicals and antimicrobials in foods. Food Chem 91: 621-632.
6. Oussalah M, Caillet S, Saucierc L, Lacroix M (2006) Antimicrobial effects of selected plant essential oils on the growth of a *Pseudomonas putida* strain isolated from meat. Meat Sci 73: 236-244.
7. Shapira R, Mimran E (2007) Isolation and characterization of *Escherichia coli* mutants exhibiting altered response to thymol. Microb Drug Resist 13: 157-165.
8. Lazar-Baker EE, Hetherington SD, Ku VV, Newman SM (2010) Evaluation of commercial essential oil samples on the growth of postharvest pathogen *Monilinia fructicola* (G. Winter) Honey. Lett Appl Microbiol 52: 227-232.
9. Glenn GM, Klamczynski AP, Woods DF, Chiou B, Orts WJ et al. (2010) Encapsulation of plant oils in porous starch microspheres. J Agric Food Chem 58: 4180-4184.
10. FAO/WHO (2008) Microbiological hazards in fresh fruits and vegetables, Microbiological Risk Assessment Series Food and Agriculture Organization of the United Nations/World Health Organization, Rome (Italy).
11. Trombetta, D, Castelli F, Sarpietro MG, Venuti V, Cristani M et al. (2005) Mechanisms of antibacterial action of three monoterpenes. Antimicrob Agents

Chemother 49: 2474-2478.

12. Hamoud R, Zimmermann S, Reichling J, Wink M (2014) Synergistic interactions in two-drug and three-drug combinations (tholoi, EDTA and vancomycin) against multi drug resistant bacteria including *E. coli.* Phytomedicine 21: 443-447.
13. Langeveld WT, Veldhuizen EJ, Burt SA (2014) Synergy between essential oil components and antibiotics: a review. Crit Rev Microbiol 40: 76-94.
14. Nieddua M, Rassua G, Boattoa G, Bosib P, Trevisi P, et al. (2014) Improvement of thymol properties by complexation with cyclodextrins: In vitro and in vivo studies. Carbohydr Polym 102: 393-399.
15. Lawrence BM (2013) The story of India's mint oils and menthol. Perfumer Flav 38: 26-35.
16. Patel T, Ishiuji Y, Yosipovitch G (2007) Menthol: a refreshing look at this ancient compound. J Am Acad Dermatol 57: 873-878.
17. Kolassa N (2013) Menthol differs from other terpenic essential oil constituents. Regul Toxicol Pharm 65: 115-118.
18. Kamatou GP, Vermaak I, Viljoen AM, Lawrence BM (2013) Menthol: A simple monoterpene with remarkable biological properties. Phytochemistry 96: 15-25.
19. Myers R (2003) The basics of chemistry. Greenwood Press, Westport, Connecticut, London.
20. Popp FA, Gu Q, Li KH (1994) Biophoton emission: experimental background and theoretical approaches. Mod Phys Lett B 8: 1269.
21. Popp FA, Chang JJ, Herzog A, Yan Z, Yan Y (2002) Evidence of non-classical (squeezed) light in biological systems. Phys Lett 293: 98-102.
22. Cohen S, Popp FA (2003) Biophoton emission of the human body. Indian J Exp Biol 41: 440-445.
23. Benor DJ (2002) Energy medicine for the internist. Med Clin North Am 86: 105-125.
24. Jonas WB, Crawford CC (2003) Science and spiritual healing: a critical review of spiritual healing, "energy" medicine, and intentionality. Altern Ther Health Med 9: 56-61.
25. Trivedi MK, Patil S, Tallapragada RM (2013) Effect of biofield treatment on the physical and thermal characteristics of vanadium pentoxide powders. J Material Sci Eng S11: 001.
26. Trivedi MK, Patil S, Tallapragada RM (2013) Effect of biofield treatment on the physical and thermal characteristics of Silicon, Tin and Lead powders. J Material Sci Eng 2: 125.
27. Trivedi MK, Patil S, Tallapragada RM (2014) Atomic, Crystalline and Powder Characteristics of Treated Zirconia and Silica Powders. J Material Sci Eng 3: 144.
28. Trivedi MK, Patil S, Tallapragada RMR (2015) Effect of biofield treatment on the physical and thermal characteristics of aluminium powders. Ind Eng Manag 4: 151.
29. Shinde V, Sances F, Patil S, Spence A (2012) Impact of biofield treatment on growth and yield of lettuce and tomato. Aust J Basic Appl Sci 6: 100-105.
30. Sances F, Flora E, Patil S, Spence A, Shinde V (2013) Impact of biofield treatment on ginseng and organic blueberry yield. Agrivita J Agric Sci 35: 22-29.
31. Lenssen AW (2013) Biofield and fungicide seed treatment influences on soybean productivity, seed quality and weed community. Agricultural Journal J 8: 138-143.
32. Trivedi M, Patil S (2008) Impact of an external energy on *Staphylococcus epidermis* [ATCC –13518] in relation to antibiotic susceptibility and biochemical reactions – An experimental study. J Accord Integr Med 4: 230-235.
33. Trivedi M, Patil S (2008) Impact of an external energy on *Yersinia enterocolitica* [ATCC –23715] in relation to antibiotic susceptibility and biochemical reactions: An experimental study. Internet J Alternative Med 6: 2.
34. Trivedi M, Bhardwaj Y, Patil S, Shettigar H, Bulbule A (2009) Impact of an external energy on *Enterococcus faecalis* [ATCC – 51299] in relation to antibiotic susceptibility and biochemical reactions – An experimental study. J Accord Integr Med 5: 119-130.
35. Patil SA, Nayak GB, Barve SS, Tembe RP, Khan RR (2012) Impact of biofield treatment on growth and anatomical characteristics of *Pogostemon cablin* (Benth.). Biotechnology 11: 154-162.
36. Altekar N, Nayak G (2015) Effect of Biofield Treatment on Plant Growth and Adaptation. J Environ Health Sci 1: 1-9.
37. Bhateja SK (1983) Radiation-induced crystallinity changes in linear polyethylene. J Polym Sci 21: 523-536.
38. Takanaga M, Yamagata K (1980) Cold crystallization of polytetrafluoroethylene by irradiation. J Polym Sci Phys 18: 1643-1650.
39. Fisher WK, Corelli JC (1981) Effect of ionizing radiation on the chemical composition, crystalline content and structure, and flow properties of polytetrafluoroethylene. J Polym Sci Chem 19: 2465-2493.
40. Wijesinghe WP, Mantilaka MM, Premalal EV, Herath HMU, Mahalingam S, et al. (2014) Facile synthesis of both needle-like and spherical hydroxyapatite nanoparticles: Effect of synthetic temperature and calcination on morphology, crystallite size and crystallinity. Mater Sci Eng C Mater Biol Appl 42: 83-90.
41. Lazic S, Zec S, Miljevic N, Milonjic S (2001) The effect of temperature on the properties of hydroxyapatite precipitated from calcium hydroxide and phosphoric acid. Thermochim Acta 374: 13-22.
42. Carballo LM, Wolf EE (1978) Crystallite size effects during the catalytic oxidation of propylene on Pt/γ-Al_2O_3. J Catal 53: 366-373.
43. Kang L, Jun HW, McCall JW (2000) Physicochemical studies of lidocaine–menthol binary systems for enhanced membrane transport. Int J Pharm 206: 35-42.
44. Szabo L, Cik G, Lensy J (1996) Thermal stability increase of doped poly (hexadecylthiophene) by γ-radiation. Synt Met 78: 149-153.
45. Mathur A, Prasad GBKS, Rao N, Babu P, Dua VK (2011) Isolation and identification of antimicrobial compound from *Mentha piperita*. Rasayan J Chem 4: 36-42.